

Roll Moment Characteristics of Asymmetric Tangential Leading-Edge Blowing on a Delta Wing

D. I. Greenwell* and N. J. Wood†

University of Bath, Bath BA2 7AY, England, United Kingdom

The concept of asymmetric tangential leading-edge blowing (TLEB) for the control of separated vortical flows is presented. Experimental results for the development of roll moment on a delta wing at high angles of attack and sideslip have been obtained and the underlying flow mechanisms examined. The application of the concept as an aircraft control system is discussed.

Nomenclature

A_j	= slot exit area
C_l	= wing roll moment coefficient
C_p	= pressure coefficient
C_{pmin}	= minimum pressure coefficient (vortex suction peak)
C_μ	= blowing moment coefficient
c	= wing root chord
\dot{m}	= jet mass flow
q	= freestream dynamic pressure
r	= leading-edge radius
S	= wing reference area
s	= wing semispan
t	= wing thickness
V_j	= jet exit velocity
V_∞	= freestream velocity
y	= spanwise coordinate
α	= angle of attack
β	= sideslip angle
Δp	= difference between plenum chamber and freestream static pressure
θ	= pitch angle
Λ	= leading-edge sweep
λ	= wing taper ratio
ρ	= freestream density
ϕ	= roll angle

Subscripts

L	= left side blowing only
R	= right side blowing only
T	= total wing blowing, $L + R$

Introduction

THE advantages for combat aircraft of extended operation in the high-angle-of-attack flight regime are considerable,¹ with the potential for "point and shoot" or agile "reduced time to turn" maneuvers. However, the development of control forces in this regime remains a significant challenge, with extensive regions of asymmetric separated unsteady flow over wing, tail, and fuselage, generating nonlinear instabilities (wing rock, nose slice, etc.²), and at the same time reducing the effectiveness of conventional control surfaces. It is there-

fore of interest to investigate new mechanisms for the production of pitch, yaw, and roll moments such that aircraft can be trimmed or maneuvered at extreme angles of attack and sideslip, or that instabilities and nonlinearities can be corrected.

Recent experimental^{3,4} and numerical^{5,6} investigations into the concept of tangential leading-edge blowing (TLEB) for the control of separated vortical flows on delta wings have demonstrated a capability for yaw and roll moment generation at high angles of attack. This article will focus on the static roll moment characteristics of asymmetric TLEB, describing the results of further experimental studies and identifying the mechanisms associated with the vortical flow control. The implications for vehicle application will be discussed.

Tangential Leading-Edge Blowing

The concept of flow control by tangential leading-edge blowing is based on the phenomenon of Coanda jet attachment to convex surfaces.⁷ The high curvature of the surface enhances the entrainment rate of the jet, induces strong suction under the jet, and accelerates the transfer of momentum from the jet to the outer flow. This can be used to delay the separation of an outer flow, and in some instances produce a global modification of the flowfield. Examples of the application of Coanda wall jets include circulation control aerofoils,⁸ control of wind-tunnel boundary layers,⁹ and blown trailing-edge flaps.¹⁰

Recently, wall jet blowing has been applied to the control of the crossflow separation on rounded leading-edge delta wings¹¹ (Fig. 1). The wall jet momentum now controls the strength and location of the leeside vortex pair. Previous results¹² have shown this particular application also capable of removing a vortex burst from the wing, in a process analogous to reducing the "effective" angle of attack of the vortical flow.

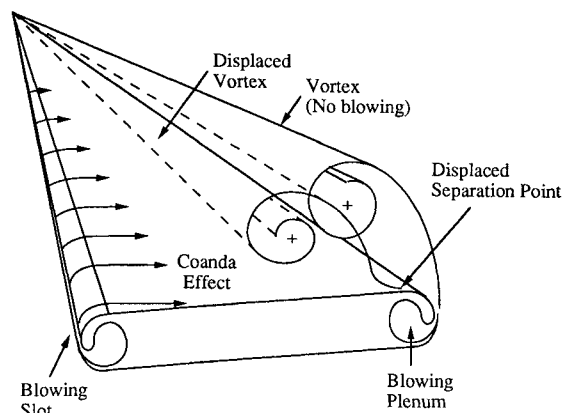


Fig. 1 Tangential leading-edge blowing.

Received July 31, 1992; revision received Nov. 30, 1992; accepted for publication Dec. 3, 1992; presented as Paper 93-0052 at the AIAA 31st Aerospace Sciences Meeting, Reno, NV, Jan. 11-14, 1993. Copyright © 1992 by the American Institute of Aeronautics and Astronautics, Inc. All rights reserved.

*Research Officer, School of Mechanical Engineering.

†Senior Lecturer, School of Mechanical Engineering. Member AIAA.

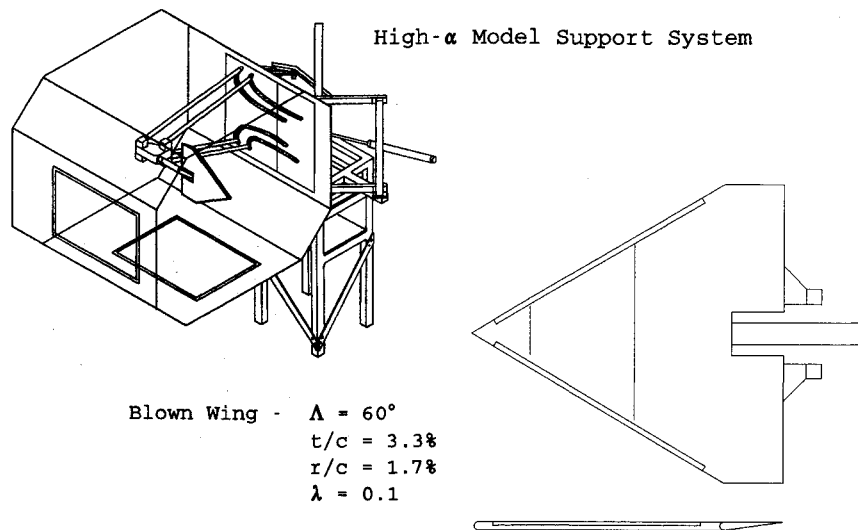


Fig. 2 Blown delta wing model in the University of Bath 2.1- \times 1.5-m low-speed wind tunnel.

Experimental Apparatus

Full details of the experimental setup are given in Ref. 13. A full-span cropped 60-deg delta wing was sting mounted in the University of Bath 2.1- \times 1.5-m low-speed wind tunnel (Fig. 2). The model support rig had a pitch angle range of -5 to 85 deg; coupled with a roll angle capability of ± 180 deg (about the model axis), this gave a ± 90 -deg range in both angle of attack and sideslip angle. The pantograph-type pitch mechanism maintained the wing on the tunnel centerline, thus minimizing asymmetric blockage effects.

The wing was of constant thickness, approximately 3% at the root chord with a circular leading-edge profile. Maximum blockage ratio was approximately 5%, keeping interference effects to a minimum. Tangential blowing slots extended over the majority of the swept leading edges, supplied from separate internal plenum chambers, with slot height varying conically from 0.1 mm near the apex to 0.5 mm at the tip. Mean slot height/radius ratio was 0.05. This slot configuration has previously been shown to give more readily interpreted results.^{11,12}

Normal force and roll moment data were provided by a sting balance integral with the model support system. Four rows of pressure tapings at 20, 35, 50, and 65% chord gave upper-surface and leading-edge pressure distributions, while blowing plenum chamber pressures were measured using two internal pressure transducers. An indication of lower-surface pressure variations was obtained by inverting the wing. No corrections were applied to the experimental data. Test Reynolds numbers were around 1.1×10^6 , based on wing root chord, corresponding to a freestream velocity of 30 ms^{-1} .

C_μ is defined as the nondimensional form of the jet momentum

$$C_\mu = \dot{m}V_j/qS$$

With the simplifying assumptions of incompressible flow and the local exit static pressure equal to freestream static, this becomes

$$C_\mu = 2(A_j/S)(V_j/V_\infty)^2$$

where

$$V_j^2 = 2(\Delta p/\rho)$$

Effect of Blowing on the Vortical Flowfield

The effects of symmetric blowing on the upper-surface pressure distribution on a delta wing have been previously

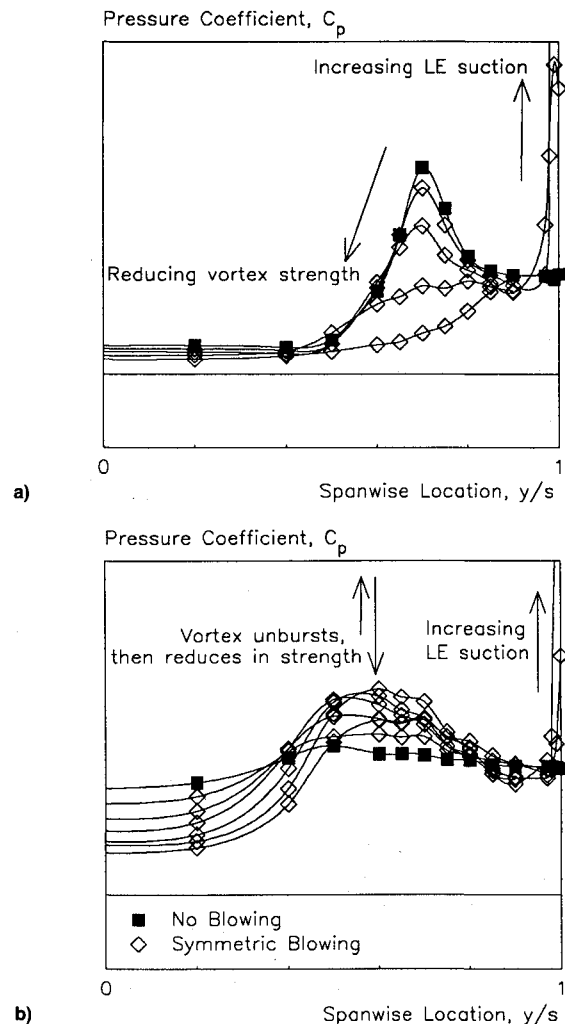


Fig. 3 Typical effect of symmetric blowing on delta wing upper-surface pressures: a) unburst vortex (pre stall) and b) burst vortex (post stall).

described¹¹ and are illustrated in Fig. 3. For an unburst vortex, the inboard movement of the leading-edge separation point with blowing results in a reduction in vortex strength (Fig. 3a). If the vortex is burst, blowing also moves the burst point aft, giving an initial increase in the suction peak at a given chordwise location as the burst moves past, followed by a

reduction as before (Fig. 3b). At high blowing levels, the leading-edge vortex is completely suppressed, with the separation point displaced to the wing centerline and the pressure distribution approaching the fully attached "RT Jones" slender wing case. The overall result of symmetric blowing is analogous to reducing the effective angle of the vortical flow.¹³

With asymmetric blowing (Fig. 4), a strong coupling of the vortical flow is apparent.³ At low angles of attack (Fig. 4a), with both vortices unburst, the blown vortex reduces in strength in a similar manner to the symmetric case, while the opposite unblown vortex is unaffected. At high prestall angles of attack, with both vortices burst, but coherent vortical flow still present (Fig. 4b), a reversal of operation occurs, in that blowing on one side initially unbursts the opposite vortex. This unblown vortex increases in strength with blowing up to a maximum, and thereafter remains constant. The blown vortex behavior resembles the symmetric case, with an initial increase in strength as it unbursts, followed by a subsidence into fully attached flow. At poststall angles of attack (Fig. 4c), the wing flow is fully separated. Blowing on the right side results in the re-establishment of coherent vortical flow on both sides, at about the same rate.

Reference 3 notes from flow visualization that the effect of asymmetric blowing is to shift the wing "plane of symmetry" (for want of a better term) away from the blown leading edge, in a manner similar to the effect of sideslip. This resemblance is reinforced by the effect of sideslip on burst location¹⁴ and by the similarity of blowing and sideslip-induced roll moments,¹³ in particular the "roll reversal" at high angles of attack as illustrated by Fig. 5. This figure shows roll moment coefficient contours as a function of angle of attack and right-side blowing (Fig. 5a) and sideslip angle (Fig. 5b). An "effective sideslip" analogy was expanded in Ref. 13 from a conceptual viewpoint, and it was shown that the roll moment characteristics of asymmetric blowing are consistent with an increase in "effective sweep angle" on the unblown side coupled with a reduction in "effective sweep" and vortex angle of attack on the blown side. A significant implication of this analogy is that the cross-coupling phenomenon is not merely a poststall effect as previously suggested,³ but occurs at all angles of attack at which a burst vortex is present on the wing and has the primary effect of altering burst point position on both sides of the wing.

Examination of the chordwise behavior of upper-surface pressure distributions supports the essential features of the analogy. However, the effects of sideslip and blowing on vortex strength are dissimilar, and this may be illustrated by the behavior of the magnitude of the vortex-induced suction peak C_{pmin} as angle of attack is increased (Fig. 6). Reference 15 demonstrates that vortex strength is a function of the magnitude of the suction peak and its half-width. For the relatively thick rounded leading-edge wing tested, the half-width remains effectively constant with angle of attack and/or blowing up to the onset of the burst, therefore, the suction peak magnitude is directly related to the vortex strength. The onset of vortex burst is indicated by a break in the curve.

Figure 6a shows the effect of a nonzero roll angle on C_{pmin} on the right-side wing half as angle of attack is varied. Since the roll angle is about the geometric body axis, this corresponds to angle of sideslip, which increases with angle of attack (for fixed roll angle). Increasing effective leading-edge sweep ($\phi = -20$ deg) reduces the strength of the vortex before the burst, delays the burst, and gives a more abrupt break. Reducing effective sweep increases preburst strength and hastens burst onset.

Figure 6b shows the effects of symmetric and asymmetric blowing on C_{pmin} on both sides of the wing. The result of symmetric blowing is a simple shift to the right relative to the baseline no blowing curve, consistent with the effective vortex angle-of-attack analogy. For asymmetric (one-sided) blowing, the results are more complex. On the blown side of the wing, the curve shifts to the right as for the symmetric case, but

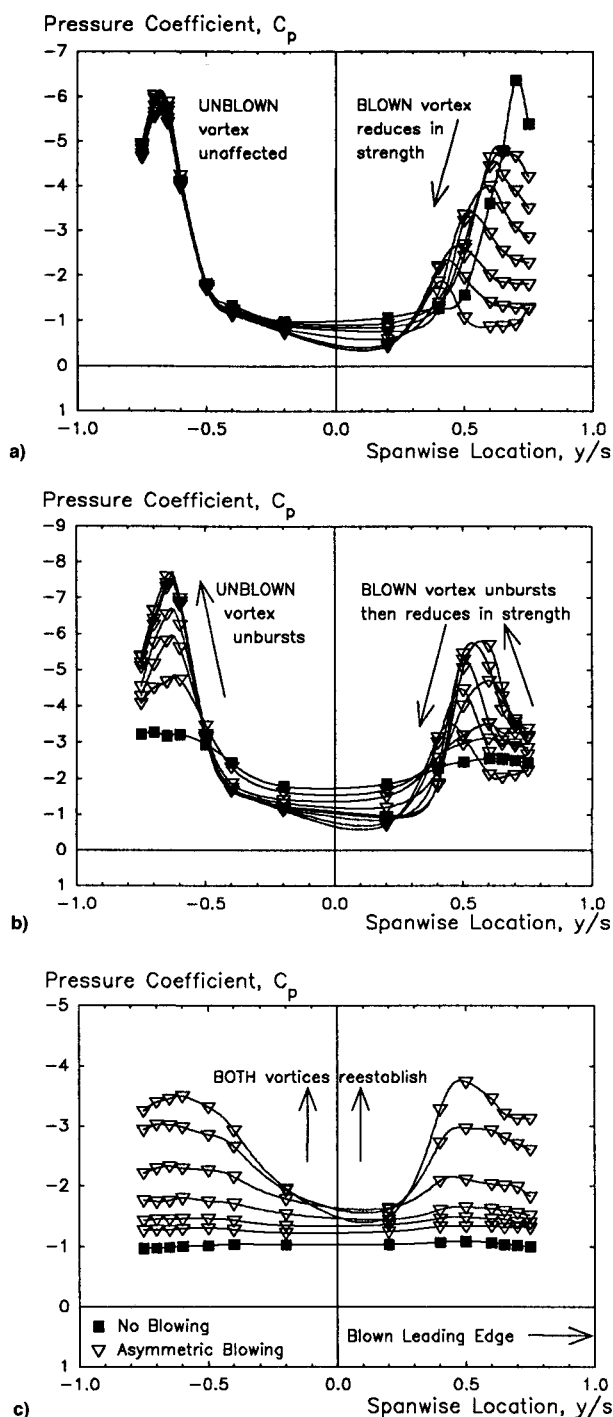


Fig. 4 Effect of increasing asymmetric (one-sided) blowing on upper-surface pressure distribution ($x/c = 0.2$, $\alpha = 30, 40, 50$ deg): a) low angles of attack, b) prestall angles of attack, and c) poststall angles of attack.

shows an earlier onset of vortex burst. On the unblown side, preburst vortex strength and the postburst trend are unaffected; the sole influence of blowing on one side on the flow on the other side of the wing is to delay the vortex burst.

Thus, the essential difference between the effects of sideslip and asymmetric blowing (on the opposite side) on a leading-edge vortex is that sideslip results in a change in leading-edge sweep, and therefore, a change in both vortex strength and burst location, while opposite blowing affects the burst location only.

This result in itself is possibly worthy of further investigation, since it provides evidence of a strong coupling between leading-edge vortices even at relatively low sweep angles and angles of attack. Previous studies have shown the sensitivity

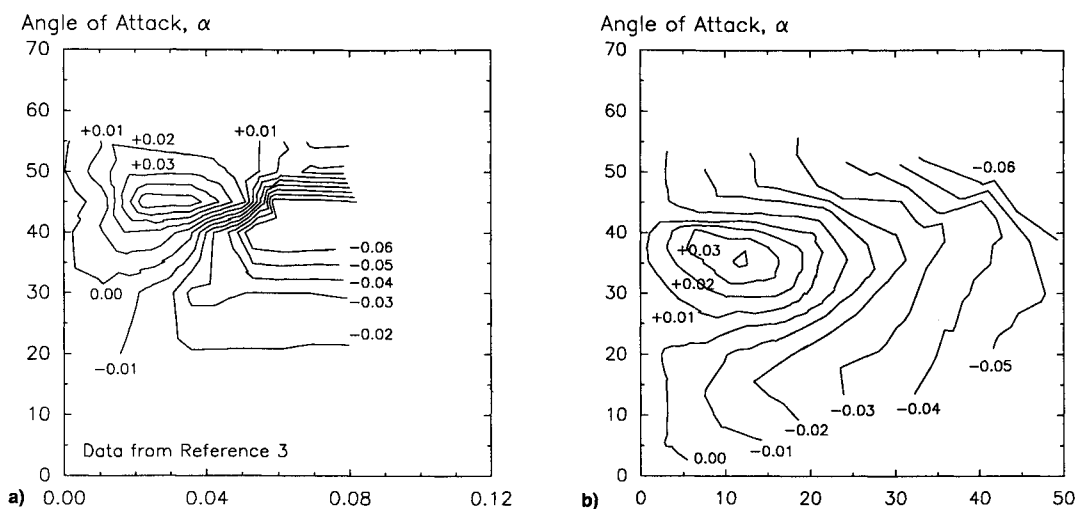
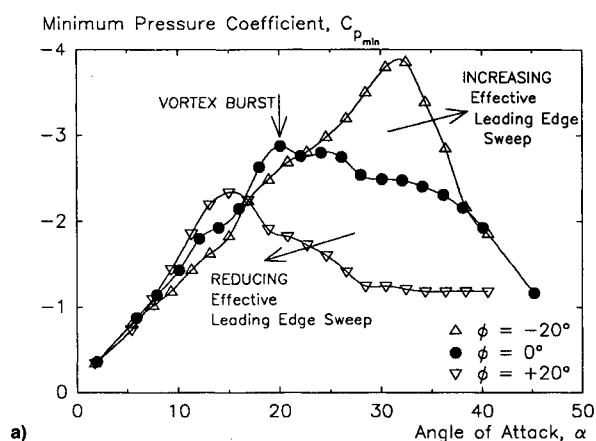


Fig. 5 Roll moment coefficient for a 60-deg delta wing¹³ vs angle of attack: a) asymmetric (right side) blowing and b) sideslip angle.



a)

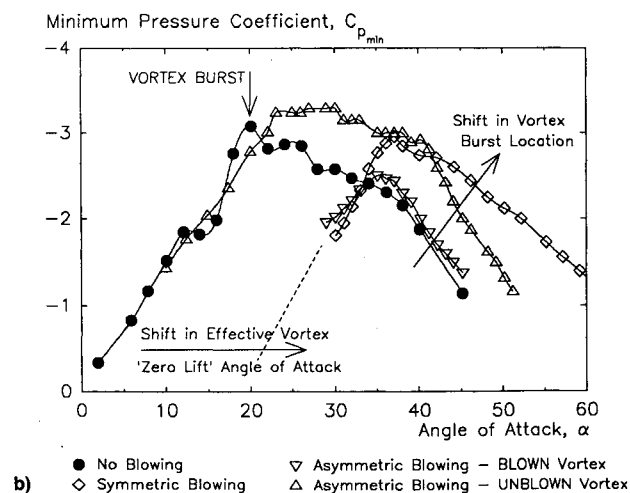


Fig. 6 Magnitude of vortex-induced suction peak ($x/c = 0.5$): a) effect of roll angle and b) effect of TLEB.

of the burst location to leading-edge profile and downstream blockage,¹⁶ but an interaction between leading-edge vortices has not been considered.

Roll Moment Characteristics

The result of this strong vortex coupling can be seen in the complex nonlinear roll moment characteristics of asymmetric blowing.

Figure 7 shows the effect of increasing angle of attack at constant asymmetric blowing levels on roll moment at zero roll angle. These results may be compared with the data of

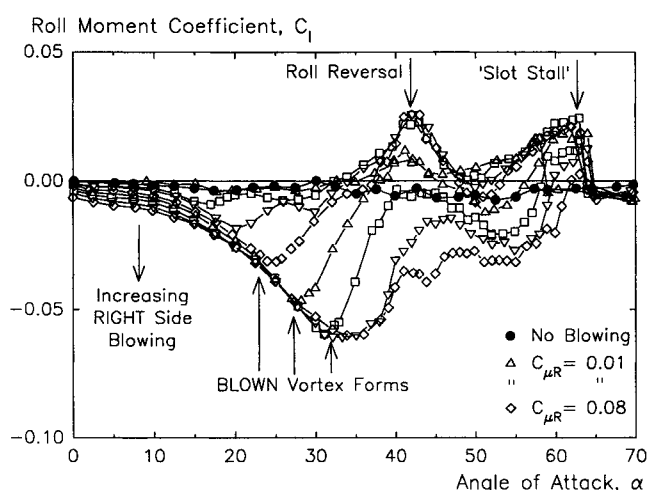


Fig. 7 Roll moment due to asymmetric blowing—increasing angle of attack at constant right-side blowing levels ($C_{\mu R} = 0.0-0.08$).

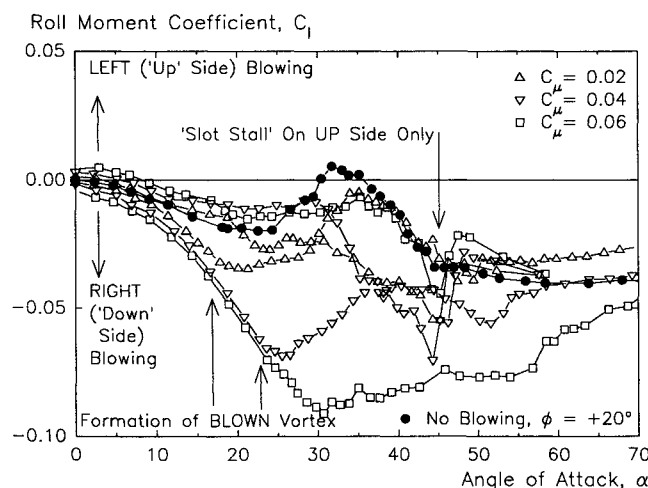


Fig. 8 Roll moment due to asymmetric blowing with nonzero roll angle ($\phi = +20$ deg, $C_{\mu L} = 0.0-0.06$, $C_{\mu R} = 0.0-0.06$).

Ref. 3 for a similar planform tested at Stanford University, as replotted in Fig. 5. Overall roll moments are similar, despite the considerably greater thickness and tunnel blockage of the Stanford wing. Significant features of the curves are the roll reversal at the stall and a complete loss of control power above 60 deg; these will be discussed in more detail later.

The effects of nonzero roll angle are essentially similar to the zero roll case, with an initial asymmetry in burst location and postburst vortex characteristics due to the different effective leading-edge sweep angles. The general effects may be illustrated by the examination of results for one roll angle, +20 deg, with right and left side asymmetric blowing (Fig. 8). A significant asymmetry in control power has developed. Stabilizing (negative, out of roll) moments have increased, while maneuver (positive, into roll) moments have reduced over the whole angle-of-attack range. This asymmetry was also seen in Ref. 4. The maximum roll angle at which the wing could be trimmed was between 10–15 deg, depending on angle of attack.

Roll Moment Generation

To understand the underlying mechanisms for these complex roll characteristics, the individual contributions of regions of the flowfield need to be isolated. For this purpose, an analysis of the pressure-integrated local roll moment at 50% chord was carried out. Total local roll moment at this location was found to correlate reasonably well with the measured total wing moments, presumably due to the very rapid motion of the burst over the aft half of the wing.¹⁷

Zero Roll Angle

Figure 9 illustrates a representative asymmetric blowing case, $C_{\mu R} = 0.04$, with the curve divided into five angle-of-attack regions. Corresponding local roll moment at 50% chord is shown in Fig. 10, split into vortical flow and jet-induced contributions. The jet-induced contribution is primarily from the flow around the leading edge, while the vortical contribution is from the inboard portion of the wing. Note that the onset of vortex burst is not necessarily marked by an immediate change in the vortical flow contribution; the reduction in C_{pmin} shown in Fig. 6 is counterbalanced by a rapid increase in half-width of the suction peak.

At low angles of attack (region I) the blown side vortex is completely suppressed, and the roll moment is dominated by the large contribution of the jet-induced suction, giving a "blown wing up" moment. Significantly, this roll moment is largely independent of blowing level (Fig. 7). A closer examination of the corresponding upper surface pressures show a remarkable similarity to the RT Jones potential flow pressure distribution predicted by slender wing theory, with some modification due to the finite thickness of the wing. The implication is that this roll moment is a result primarily of the jet-induced displacement of the separation point, and not directly due to the suction induced by the jet itself. The impact of leading-edge profile on this component of the roll moment

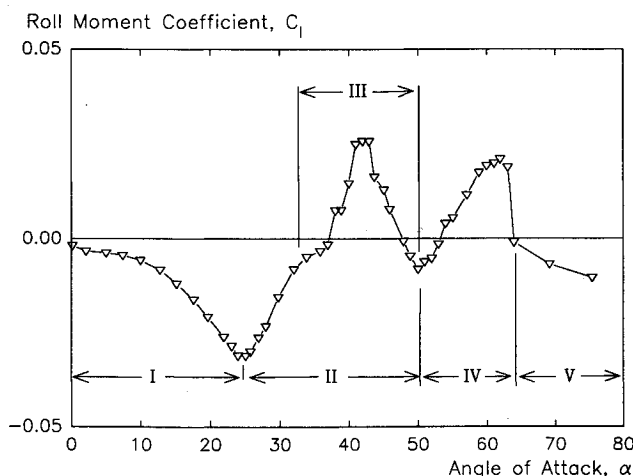


Fig. 9 Representative roll moment behavior due to right-side blowing at zero roll angle ($C_{\mu R} = 0.04$).

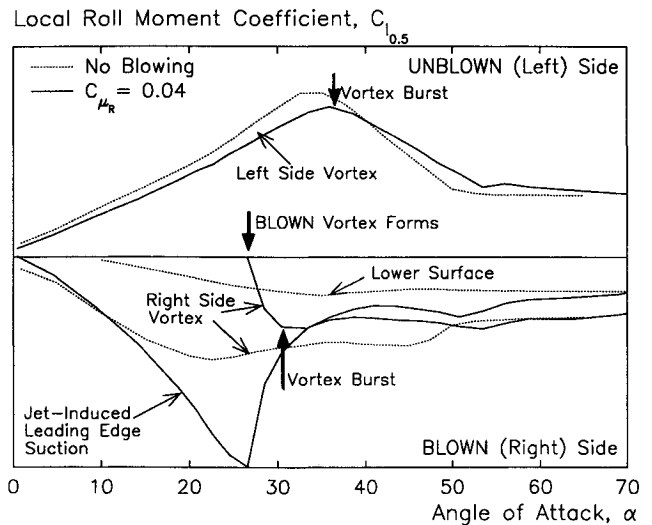


Fig. 10 Contributions to roll moment behavior due to right-side blowing at zero roll angle ($C_{\mu R} = 0.04$).

is likely to be a second-order effect; a further experimental investigation is in progress.

The overall magnitude of the roll moment is somewhat less than the levels indicated by integration of upper-surface pressures on the forward section of the wing. The most likely explanation is that on the blown side of the wing, the side-edge vortex¹⁸ is very much reduced in strength relative to the unblown side, counteracting the leading-edge suction and giving a decrease in overall roll moment in region I. This hypothesis is supported by experimental data from Ref. 18, which indicates that small changes to the tip geometry (and hence, tip flowfield) of a cropped-delta wing can generate significant roll moments.

At around 25 deg, the blown vortex re-establishes (region II), and there is an abrupt loss of the RT Jones flow component as the separation point moves rapidly from the wing centerline to near the leading edge. The overall change in normal force is small, but the reduced roll arm of the vortex-induced load results in a rapid loss of roll moment.

Within region II, a subregion III is apparent, corresponding to the presence of the vortex bursts on the wing, with the associated coupling effect. As angle of attack increases, first the unblown and then the blown vortex burst come onto the wing. The unblown burst is relatively gentle, giving a modest recovery in roll moment. However, the more abrupt lift loss shown by the blown vortex as it bursts results in a sharp further loss of roll moment to give the "roll reversal" phenomenon.

By around 50 deg the vortex bursts have reached the wing apex and the vortical flow has largely subsided (region IV). The contribution of the jet-induced flow over the forward portion of the wing is negative ("blown side up"), but is counteracted by the loss of lift at the tip noted in region I.

At around 60 deg a phenomenon occurs which was not seen in earlier TLEB studies, but has been previously noted on circulation control aerofoils.⁸ The flow around the blown leading edge separates before the slot lip, and there is a sudden loss of blowing effectiveness. The jet-induced component vanishes and roll moment falls to practically zero (region V), with the small suction contribution of the jet itself counterbalanced by the reaction at the slot. The onset of this "slot stall" is a function of leading-edge profile, slot position, and sweep angle. In early tests a hysteresis loop was present in this region, until the lower surface boundary-layer transition was fixed using a trip parallel to the leading edge.

On the basis of this analysis, the resemblance between the effects of sideslip and asymmetric blowing on overall roll moment behavior is no more than that; a resemblance. Although both exhibit a roll-reversal effect due to an asymmetry in burst

location and in postburst vortex characteristics, the details of that asymmetry are very different. Sideslip-induced roll reversal is due to the earlier vortex burst onset on the "into wind" wing, compared with the "out of wind" wing, whereas the equivalent blown vortex burst actually occurs later than the unblown burst. The blowing-induced roll reversal phenomenon is primarily a function of the more abrupt burst behavior of the blown vortex. It is possible, therefore, that a change in wing sweep may significantly affect this occurrence; tests on the effect of sideslip suggest that the blown postburst loss in roll moment is considerably less violent for a lower effective leading-edge sweep angle. The overall effect of a less highly swept wing (e.g., 50–55 deg), may thus be to smooth out the roll reversal region.

The reduction in roll control power due to lift loss at the tip indicates that for maximum capability the slot should extend to the tip, and that the tip chord be kept to a minimum. Exploratory tests with a tip extension piece have shown the roll moment curve of Fig. 9 to be sensitive to tip shape, particularly in region I. An application of the side-edge vortex method of Ref. 18 gives a crude estimate of a 100% increase in roll power in region I for a full-length slot.

Effect of Nonzero Roll Angle

A similar analysis may be performed for the roll moment characteristics due to a nonzero roll angle. Figure 11 shows total wing roll moment for a representative roll angle of +20 deg, with blowing levels of 0.06 on the left (up, out of wind) side, and 0.04 on the right (down, into wind side). The individual local roll moment contributions at 50% chord are identified in Figs. 12 (left blowing) and 13 (right blowing). An additional factor is the presence of a stabilizing roll contribution from the underside (potential) flow.

For left (up) side blowing, the regions identified for the zero roll case have shifted considerably. At low angles of attack (region I), the jet-induced roll moment has reduced as the effective aspect ratio of the left side has reduced. On the right side, with a lower initial sweep angle, the unblown vortex bursts before the blown vortex forms, resulting in region III (burst vortices on the wing) overlapping regions I and II. The net result is that the roll reversal phenomenon occurs earlier and is less pronounced, but control power has been almost completely lost. The rapid loss in roll control power with the formation of the blown vortex (region II) occurs as for the zero roll case. However, the early onset of slot stall (as a result of the high effective sweep angle of the leading edge) pre-empts the formation of region IV; the loss of blowing effectiveness results in the flowfield returning to a fully separated flow.

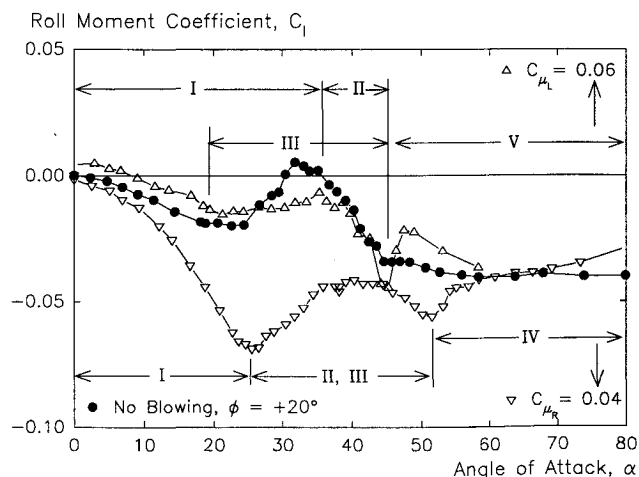


Fig. 11 Representative roll moment behavior due to left- and right-side blowing at nonzero roll angle ($\phi = +20$ deg, $C_{\mu L} = 0.06$, $C_{\mu R} = 0.04$).

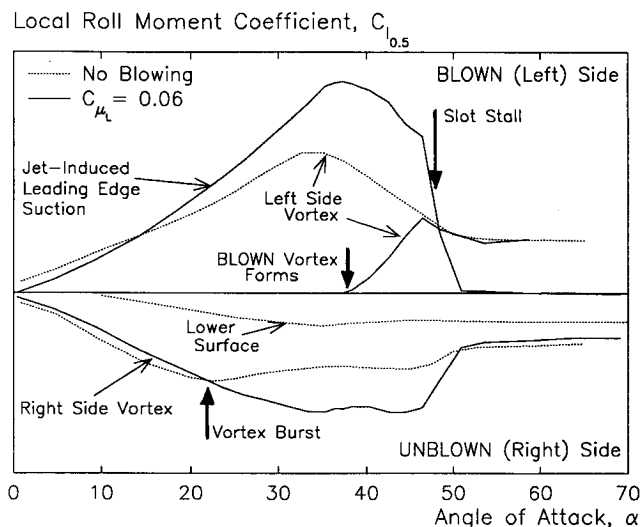


Fig. 12 Contributions to roll moment behavior due to left-side blowing at nonzero roll angle ($\phi = +20$ deg, $C_{\mu L} = 0.06$).

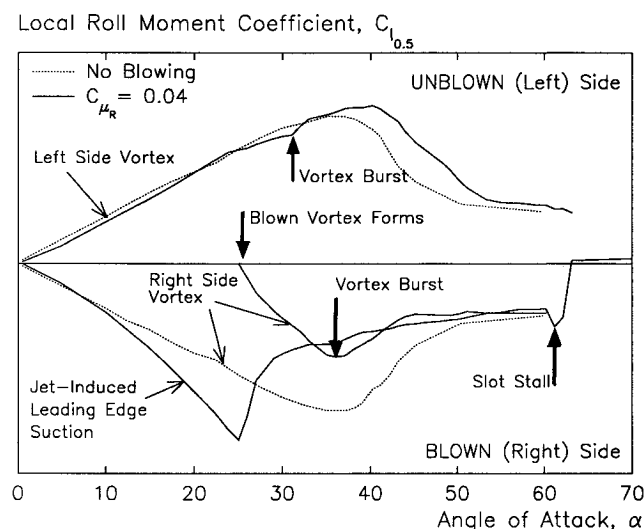


Fig. 13 Contributions to roll moment behavior due to right-side blowing at nonzero roll angle ($\phi = +20$ deg, $C_{\mu R} = 0.04$).

For right (down) side blowing, the roll moment behavior and contributions are essentially similar to those at zero roll angle, without the roll reversal. The significant differences are that the blown vortex burst is very much gentler and slightly ahead of the unblown burst, tending to smooth out the roll reversal, and that the slot stall does not occur in the angle-of-attack range tested. The delay, or suppression, of slot stall is due to the lower initial effective sweep angle of the blown leading edge, and results in very high stabilizing roll control power being maintained up to extremely high angles of attack (Fig. 8).

The cause of the overall increase in stabilizing control power and reduction in maneuver power noted above lies in the down side vortex burst behavior. The lower effective leading-edge sweep gives a generally less abrupt burst process (blown and unblown), with relatively little loss of roll moment contribution.

Considerations for Application to Flight Vehicles

Tangential leading-edge blowing has the potential to generate rolling moments in excess of the capabilities of conventional control surfaces at very high angles of attack.³ Mass flow requirements are comparable to STOVL reaction control systems; for a modern combat aircraft at the low speeds typical

of high-angle-of-attack maneuvers, scaling jet mass flow directly on C_{μ} , gives values around 20% of compressor flow. Possible increases in blowing efficiency with reduced slot height may well reduce mass flow requirements. Depending on engine rating philosophy, this level of engine bleed may not necessarily give proportional thrust losses. Interestingly, recent work on tangential forebody blowing on a full-size F18¹⁹ suggests that a more appropriate scaling function may be mass flow ratio (i.e., mass flow proportional to ρV_{∞}), rather than C_{μ} (proportional to ρV_{∞}^2), significantly reducing bleed flow requirements.

For successful application, a number of factors need to be resolved. First is the effect of leading-edge radius. Real wings have much smaller leading-edge radii than the generic flat plate wing tests reported here. Because the contributions to roll moment identified above are all essentially responses of the outer flow to a displacement of the leading-edge separation, it seems likely that the effect of further reductions in leading-edge radius will be small, as long as control of the separation location can be maintained. Some confirmation of this is given by the relatively small changes in local jet-induced roll moment coefficient with chordwise location (from 20 to 65% chord), despite the wide variation in local leading-edge radius to span ratio (7 to 2%). In this respect, the effect of reductions in surface radius on other Coanda wall jet applications has been to improve efficiency.

The effect of wing planform on the nonlinear nature of the roll moment characteristics is not known. As discussed earlier, it is possible that sweep angles of less than 60 deg may not exhibit the undesirable (from a flight control viewpoint) roll reversal phenomenon, due to a less abrupt vortex burst process. Encouragingly, a sweep angle of between 45–55 deg would in fact be more representative of current combat aircraft. The effect of tip geometry and blowing slot extent also need to be clarified, since these may be particularly significant.

In this test program, side forces and yawing moments were not measured due to balance limitations. However, from visual observation of the model behavior under test, and from the leading-edge pressure distributions, they may be significant. Any side force generated by blowing will be in an adverse direction (i.e., towards the blown side), although a drag reduction will also result from the thrust component. Integration of leading-edge pressures on the blown side at low angles of attack indicates that local side force coefficients fall off rapidly towards the rear of the wing as local thickness/span ratio reduces, while extrapolation forward to the wing apex gives a value very close to the side force predicted by slender wing theory. The implication is that for representative wing thicknesses, overall side forces will be small, although limitations of model size have as yet precluded experimental confirmation.

Finally, the dynamic behavior of transient blowing, particularly in conjunction with roll motion, requires further investigation. Initial studies of flowfield response to transient symmetric blowing (at zero roll angle)²⁰ have identified two time scales: 1) a relatively fast response (of the order of one convective length) associated with the crossflow equilibrium condition and changes in vortex strength; and 2) a slower component (5–10 convective lengths) associated with the longitudinal equilibrium of the flow and relocation of the vortex burst. At high angles of attack, where the roll moment response is a combination of jet-induced flow, asymmetric vortex strength, and asymmetric burst location, the resultant response to transient blowing is likely to be complex. A successful recent application of TLEB to the control of wing rock of a delta wing model²¹ resolved this problem by using an initial symmetric blowing level sufficient to keep the vortex burst off the wing, and removing the second, slower, response time scale. A further complication is that roll rate can in itself generate lags in vortex position, strength, and burst location,²² introducing further nonlinearities.

Experimental studies into the factors discussed above, except the effect of sweep angle, are in progress at the University of Bath, and will be reported upon in due course.

Conclusions

Experimental results suggest that tangential leading-edge blowing is an effective mechanism for controlling separated flows, including both burst and unburst vortices. Asymmetric blowing is capable of generating roll moments in excess of conventional moving surface controls at high angles of attack, although leading-edge geometry and wing planform effects and dynamic characteristics need further investigation prior to flight vehicle application.

The strong cross-coupling of the vortex burst phenomenon induces strongly nonlinear static roll moment characteristics, which would be undesirable for a flight control system, but which may be amenable to alleviation through changes in wing planform.

The effect of asymmetric blowing on the wing flowfield is qualitatively equivalent to an increase in sweep angle on the unblown wing side, and a reduction in both sweep angle and effective vortex angle of attack on the blown side. The overall roll moment characteristics of asymmetric blowing, although bearing a resemblance to the effects of sideslip, are in fact due to a quite different combination of vortex burst and strength asymmetries.

References

- ¹Chody, J. R., "Combat Aircraft Control Requirements for Agility," Paper 4, AGARD Symposium on Aerodynamics of Combat Aircraft and of Ground Effects, AGARD CP-465, Oct. 1990.
- ²Ross, A. J., "High Incidence—The Challenge to Control Systems," Lecture presented to the Royal Aeronautical Society, London, Jan. 1990.
- ³Wood, N. J., Roberts, L., and Celik, Z., "Control of Asymmetric Vortical Flows over Delta Wings at High Angles of Attack," *Journal of Aircraft*, Vol. 27, No. 5, 1990, pp. 429–435.
- ⁴Wood, N. J., "Development of Lateral Control on Aircraft Operating at High Angles of Attack," International Council of the Aeronautical Sciences 90-5.6.3, Sept. 1990.
- ⁵Yeh, D., "Numerical Simulation of the Flow Field over Delta Wings with Leading Edge Blowing," Ph.D. Dissertation, Stanford Univ., Stanford, CA, 1988.
- ⁶Craig, K., "Computational Study of the Aerodynamics and Control by Blowing of Asymmetric Vortical Flows over Delta Wings," AIAA Paper 92-0410, Jan. 1992.
- ⁷Lauder, B. E., and Rodi, W., "The Turbulent Wall Jet," *Progress in Aerospace Sciences*, Vol. 19, 1981, pp. 81–128.
- ⁸Wood, N. J., and Nielsen, J. N., "Circulation Control Airfoils as Applied to Rotary Wing Aircraft," *Journal of Aircraft*, Vol. 23, No. 12, 1986, pp. 865–875.
- ⁹Wood, N. J., Ward, S., and Roberts, L., "Wind Tunnel Boundary Layer Control by Coanda Wall Jets," AIAA Paper 89-0149, Jan. 1989.
- ¹⁰Englar, R. J., "Further Development of Pneumatic Thrust-Deflecting Powered-Lift Systems," *Journal of Aircraft*, Vol. 25, No. 4, 1988, pp. 324–333.
- ¹¹Wood, N. J., and Roberts, L., "Control of Vortical Lift on Delta Wings by Tangential Leading Edge Blowing," *Journal of Aircraft*, Vol. 25, No. 3, 1988, pp. 236–243.
- ¹²Wood, N. J., Roberts, L., and Lee, K. T., "The Control of Vortical Flow on a Delta Wing at High Angles of Attack," AIAA Paper 87-2278, Aug. 1987.
- ¹³Greenwell, D. I., and Wood, N. J., "Control of Asymmetric Vortical Flows," AIAA Paper 91-3272, Sept. 1991.
- ¹⁴McKernan, J. F., and Nelson, R. C., "An Investigation of the Breakdown of the Leading Edge Vortices on a Delta Wing at High Angles of Attack," AIAA Paper 83-2114, Aug. 1983.
- ¹⁵Greenwell, D. I., and Wood, N. J., "Determination of Vortex Burst Location on Delta Wings from Surface Pressure Measurements," *AIAA Journal*, Vol. 30, No. 11, 1992, pp. 2736–2740.
- ¹⁶Kegelman, J., and Roos, F., "Effects of Leading Edge Shape and Vortex Burst on the Flowfield of a 70° Sweep Delta Wing," AIAA Paper 89-0086, Jan. 1989.

¹⁷Wentz, W. H., and Kohlman, D. L., "Vortex Breakdown on Slender Sharp-Edged Wings," *Journal of Aircraft*, Vol. 8, No. 3, 1971, pp. 156-161.

¹⁸Lamar, J. E., "Prediction of Vortex Flow Characteristics of Wings at Subsonic and Supersonic Speeds," *Journal of Aircraft*, Vol. 13, No. 7, 1976, pp. 490-494.

¹⁹Meyn, L. A., and James, K. D., "Full-Scale High Angle of Attack Tests of an F/A-18," AIAA Paper 92-2676, June 1992.

²⁰Roberts, L., and Wood, N. J., "Control of Vortex Aerodynamics

at High Angles of Attack," Paper 12, AGARD Symposium on Aerodynamics of Combat Aircraft and of Ground Effects, AGARD CP-465, Oct. 1990.

²¹Wong, G., "Experiments in the Control of Wing Rock at High Angle of Attack Using Tangential Leading Edge Blowing," Ph.D. Dissertation, Stanford Univ., Stanford, CA, 1992.

²²Arena, A. S., and Nelson, R. C., "The Effect of Asymmetric Vortex Wake Characteristics on a Slender Delta Wing Undergoing Wing Rock Motion," AIAA Paper 89-3348, Aug. 1989.